ELSEVIER

Journal of Alloys and Compounds 356–357 (2003) 557–561

Journal of ALLOYS AND COMPOUNDS

www.elsevier.com/locate/jallcom

# Structural and electrochemical properties of amorphous rich $Mg_xNi_{100-x}$ nanomaterial obtained by mechanical alloying

M. Abdellaoui[a,*], S. Mokbli[a], F. Cuevas[b], M. Latroche[b], A. Percheron-Guégan[b], H. Zarrouk[a]

[a] *National Institute of Research and Physics–Chemistry Analyses, Technological Pole, 2020 Sidi Thabet, Tunisia*

[b] *Laboratoire de Chimie Métallurgique des Terres Rares, CNRS, 2–8 Rue Henri Dunant, F-94320 Thiais Cedex, France*

Received 24 September 2002; accepted 15 November 2002

**Abstract**

Using a planetary ball mill and starting from a mixture of $Mg_2Ni$ and Ni with a Mg atomic content ranging from 40 to 60 at.%, we have elaborated amorphous phase alloys with little quantities of residual Ni. The synthesis of the amorphous phase proceeded at 6.49 W $g^{-1}$ shock power, for milling durations ranging from 8 to 10 h for $Mg_{40}Ni_{60}$ and $Mg_{60}Ni_{40}$ samples, respectively. The best electrochemical capacity (470 mAh $g^{-1}$, equivalent of $MgNiH_{2.0}$) was obtained for the $Mg_{50}Ni_{50}$ sample synthesized in milling duration 10 times shorter than that commonly reported in the literature.



*Keywords:* Nanostructures; Hydrogen storage material; Amorphisation; Mechanical alloying; Electrochemical reaction

## 1. Introduction

In the last few years, research has turned to new materials in order to improve the specific capacity of the AB, $AB_2$ and $AB_5$ compounds (A an element forming a stable hydride and B an element forming instable hydride). Mg has a very low atomic weight and price compared to the rare earth materials. Its alloying with Ni leads to the formation of compounds which absorb and desorb the hydrogen reversibly. The $Mg_2Ni$ compound has been the most intensively investigated. However, the low desorption pressure (0.2–0.3 MPa) at a high temperature of 575 K [1,2] and the poor electrochemical cycling properties are the main reasons for the research of new compositions and new microstructural states for this system. Some recent works show that amorphous $Mg_{50}Ni_{50}$ alloys exhibit good improvement of the electrochemical properties: Liu et al. [3] showed that a pure amorphous phase was formed for $x=30$ to 60 Mg at.% when elemental powders of Mg and Ni are mechanically alloyed (MA) during 120 h. They showed that all amorphous alloys with $45 \leq x \leq 50$ Mg at.%, present a good discharge capacity of about 350 mAh $g^{-1}$ with a poor cycle life. This loss has been attributed to Mg corrosion and formation of $Mg(OH)_2$ hydroxide in KOH alkaline solution. Starting from a mixture of $Mg_2Ni$ and Ni and using a planetary ball mill during 80 h, Orimo et al. [4] elaborated some $Mg_{100-x}Ni_x$ materials. For $x=38$ and 43, they obtained a mixture of crystalline $Mg_2Ni$ and $Mg_{50}Ni_{50}$ amorphous phases and finally the formation of a pure amorphous phase $Mg_{50}Ni_{50}$ for $x=50$. The hydrogen absorption capacity was maximum for $x=50$ reaching 2.2 wt.% and corresponding to the hydride $MgNiH_{1.9}$. Tarashita et al. [5] showed that $Mg_{50}Ni_{50}$ amorphous phase was formed by MA for 25 h starting from $Mg_2Ni$ and Ni. The weight hydrogen desorption capacity was equal to 1.8 wt.%. The amorphous state leads to the decrease of the desorption temperature (400 K) as compared to that of the $Mg_2Ni$ compound (640 K). Lenain et al. [6] have also synthesized $Mg_{50}Ni_{50}$ amorphous materials by milling Mg and Ni in the atomic proportion 1:1 for 80 h. For the first cycle, the electrochemical discharge capacity was equal to 500 mAh $g^{-1}$ but decreases to 120 mAh $g^{-1}$ after 20 cycles due to the formation of $Mg(OH)_2$ hydroxide. Sun et al. [7] have prepared amorphous phases starting from $Mg_2Ni$ and Ni with composition $MgNi_x$ ($x=1$ and 1.14). a-MgNi and a-$MgNi_{1.14}$ phases have electrochemical capacities of 336 mAh $g^{-1}$ for the first cycle. This capacity decreases with the cycle number keeping a larger capacity for the a-$MgNi_{1.14}$ phase. Nohara et al. [8], from the milling of Mg and Ni for 36 h, have

*Corresponding author. Tel.: +216-71-537-666; fax: +216-71-537-767.

*E-mail address:* mohieddine.abdellaoui@inrap.rnrt.tn (M. Abdellaoui).

0925-8388/03/$ – see front matter 
doi:10.1016/S0925-8388(03)00119-1

synthesized a pure $Mg_{50}Ni_{50}$ amorphous phase. For the first cycle, the amorphous phase has a capacity of 480 mAh $g^{-1}$.

In this work, we try to optimize the mechanical alloying process to elaborate pure $Mg_xNi_{100-x}$ amorphous phase starting from a mixture of $Mg_2Ni$ and Ni. Also, we try to obtain the relationship between the mechanical alloying conditions and the microstructural state of the end product and the correlation between the microstructural state and the electrochemical absorption properties.

## 2. Experimental details

Samples were mechanically alloyed (MA) with a Fritsch Pulverisette P7 planetary ball mill. A 1.5-g amount of a powder mixture of Ni and $Mg_2Ni$ with Mg atomic content ranging from 40 to 60 at.% was introduced to a cylindrical steel container of 45 ml capacity. The container was loaded under an Ar atmosphere with 30 balls (diameter=7 mm, mass=1.5 g) with a balls to powder weight ratio equal to 30:1. The containers were sealed allowing perfect air tightness. MA was performed at intensity 6 which corresponds to $0.12 \cdot 10^{-1}$ J/shock kinetic shock energy, 607.5 Hz shock frequency and 6.49 W $g^{-1}$ shock power [9,10]. The alloying duration was varied until the formation of pure amorphous phase.

Small amounts of the MA powder were extracted from time to time from the container for X-ray diffraction (XRD) analysis. XRD patterns were obtained using a ($\theta$–$2\theta$) Philips or Bruker diffractometer with Cu K$\alpha$ radiation ($\lambda$=0.15406 nm). The ABFfit program [11,13] was used in order to analyze the XRD patterns and to obtain the position, the intensity and the full width at half maximum of the various peaks.

To study the electrochemical discharge capacity, a small quantity of the synthesized alloys (40–90 mg) was mixed with black carbon and PTFE in the ratio 87:5:8, respectively. This composite electrode material was pressed on a Ni grid to form the negative electrode. The positive electrode was made of Ni-oxyhydroxide/dihydroxide. The alkaline solution was 8 M KOH. To reach the theoretical maximum electrochemical capacity, the electrode was charged for 5 h at a C/5 regime (i.e. full capacity C in 5 h) and discharged at the same regime down to a cut off potential of 0.9 V between the two electrodes.

## 3. Results and discussion

### *3.1. End product structure as function of the mechanical alloying conditions*

Fig. 1 shows the XRD patterns of MA $Mg_xNi_{100-x}$ alloys for $40 \leq x \leq 60$ Mg at.% for different milling times. Whatever the Mg content, the crystalline peaks of the $Mg_2Ni$ phase disappear firstly and a halo was formed at low $2\theta$ position (close to 40°). This halo becomes wider and its intensity becomes larger when the milling time increases. When the stationary state is reached, the alloy is formed by an amorphous phase with some residual Ni. To reach the stationary state, milling time increases when increasing Mg content. It ranges from 8 h 15 min for the $Mg_{40}Ni_{60}$ sample to 9 h 55 min for the $Mg_{60}Ni_{40}$ sample. Fig. 2 gives the variation, as function of milling duration, of the ratio of amorphous phase halo intensity to the sum of the (111) Ni crystalline peak and the amorphous phase halo intensities.

Abdellaoui et al. [9,10] stated that for a given sample composition the microstructure of the stationary state as well as the kinetics of the intermediary transformations were governed only by the injected shock power given by the product of the kinetic shock energy by the shock frequency ($P$ [W]=$E_c$ [J $hit^{-1}$]×$f$ [Hz]). Nevertheless, the proportion of the intermediary phases formed is a function of the accumulated energy defined as the product of the injected shock power by the milling duration ($E$ [W h]=$P$ [W]×$\Delta t$ [h]). In other words, if the injected shock power is maintained constant, this proportion only depends on the alloying duration. In this work, all samples were synthesized at an injected shock power of 6.49 W $g^{-1}$ of material.

As can be seen from Fig. 2 the amorphous phase formation kinetic decreases with increasing Mg content. As has been reported in our previous work [9], the injected shock power in mechanical alloying phase transformation is similar to the activation energy in conventional phase transformation. In this work, as we operate with constant injected shock power, the kinetic of amorphous phase formation reflects the easiness of this reaction as a function of sample concentration. Thus, the activation energy for the crystalline to amorphous phase transformation is lower when increasing the Ni content.

Fig. 3 shows the variation of the amorphous phase first near neighbor distance (calculated from the $2\theta$ halo position on the basis of the Bragg law [12,14]) as a function of the sample composition for the corresponding stationary states. The amorphous phase near neighbor distance increases when increasing the Mg atomic content. As the stationary state is formed almost by a pure amorphous phase, the increase of the initial Mg content leads to its enrichment with Mg. As the Ni atomic radius (1.24 Å) is less than that of Mg (1.60 Å), this result can be explained by a homogeneous and statistical replacement of the Ni atoms by the Mg ones in the amorphous state. The first near neighbor distance (the specific parameter of the amorphous phase) varies linearly with increasing the Mg content $x$, at least in the range 40–55 at.% following a Vegard-type law.

This Vegard-type law has been previously reported by Gaffet [15] in Ni–Zr amorphous alloys obtained by mechanical alloying. When Mg content is higher than 55

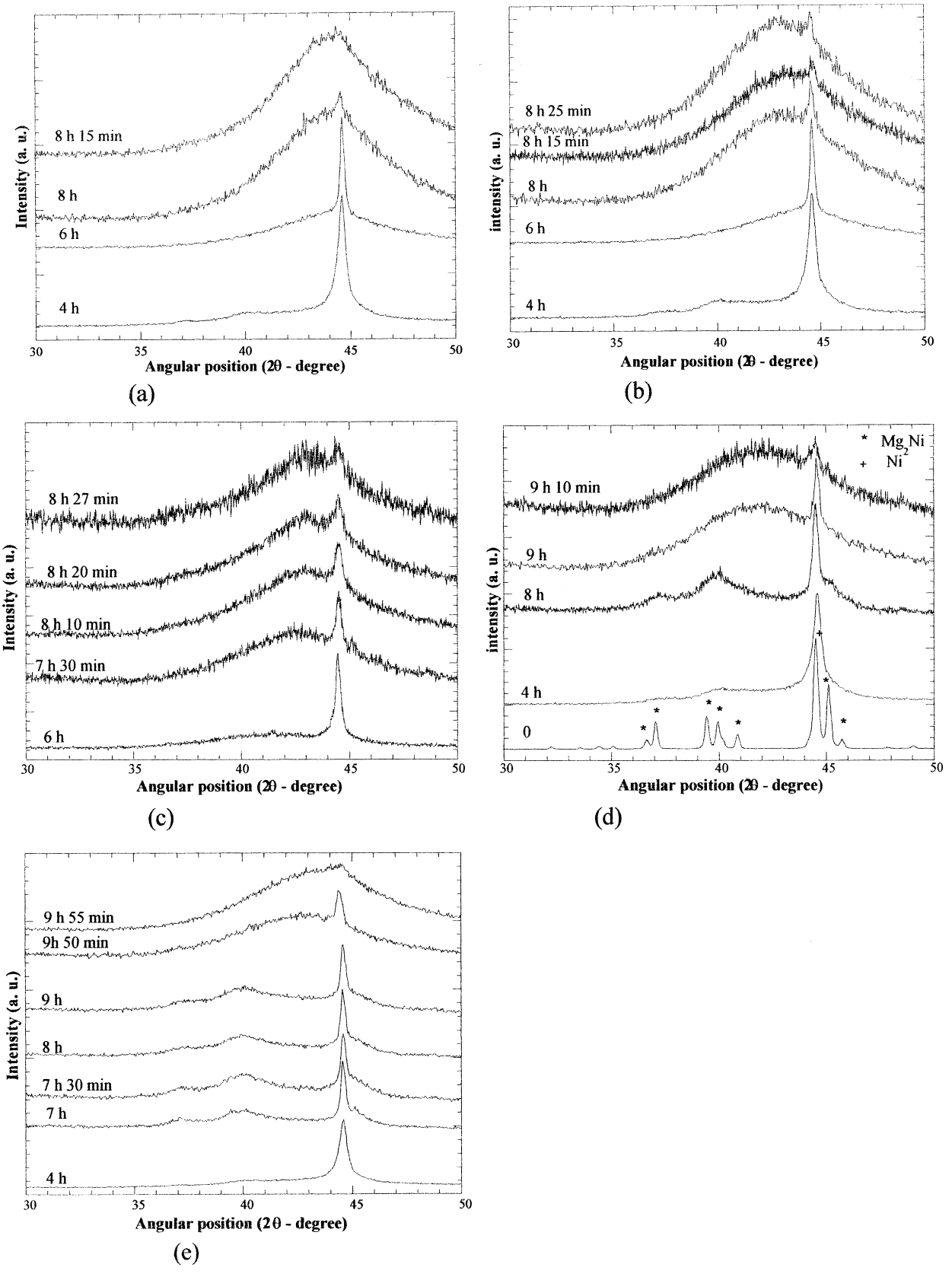


Fig. 1. XRD patterns of mechanically alloyed $Mg_xNi_{100-x}$ alloys with (a) $x=40$, (b) $x=45$, (c) $x=50$, (d) $x=55$ and (e) $x=60$ synthesized at different mechanical alloying durations.

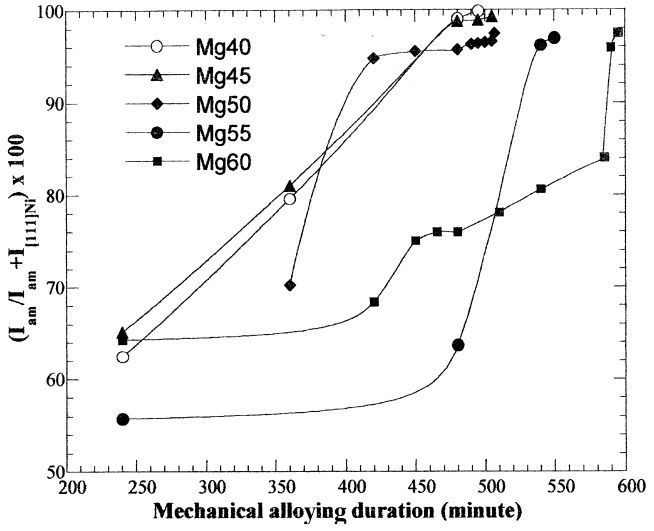


Fig. 2. Variation of the ratio of amorphous phase halo intensity to the sum of the (111) Ni crystalline peak and the amorphous phase halo intensities.

at.% we assume that the Ni atoms replacement is no longer homogeneous and the first near neighbor distance does not follow a linear variation any more. By optimization of the mechanical alloying process, the milling durations used in our work to obtain almost a pure amorphous phase were 8 h 15 min, 8 h 25 min, 8 h 27 min, 9 h 10 min and 9 h 55 min for, respectively, 40, 45, 50, 55 and 60 Mg at.% samples. The highest milling duration used is lower than those used by Liu et al. [3] (120 h), Orimo et al. [4] (80 h), Lenain et al. [6] (80 h), Sun et al. [7] (70 h), Nohara et al. [8] (36 h) and Tarashita et al. [5] (25 h).

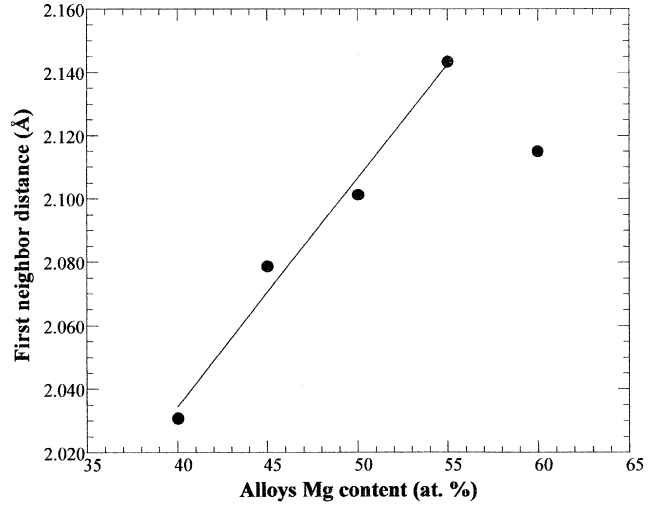


Fig. 3. Variation of the amorphous phase first near neighbor distance as a function of the sample composition for the corresponding stationary states.

### 3.2. Electrochemical properties

Fig. 4a shows the variation of the electrochemical capacity of the different synthesized samples versus the number of cycles. It can be observed that whatever the cycle number is, $Mg_{50}Ni_{50}$ has the highest capacity and $Mg_{40}Ni_{60}$ has the lowest one. For each composition, increasing the cycle number increases the electrochemical capacity to reach a maximum after four or five cycles and then decreases for upper cycle numbers. The best electrochemical capacities reached for $x=40$ to $x=60$ are, respectively, 294, 419, 470, 397 and 371 mAh $g^{-1}$.

Fig. 4b gives the variation, as function of the Mg atomic

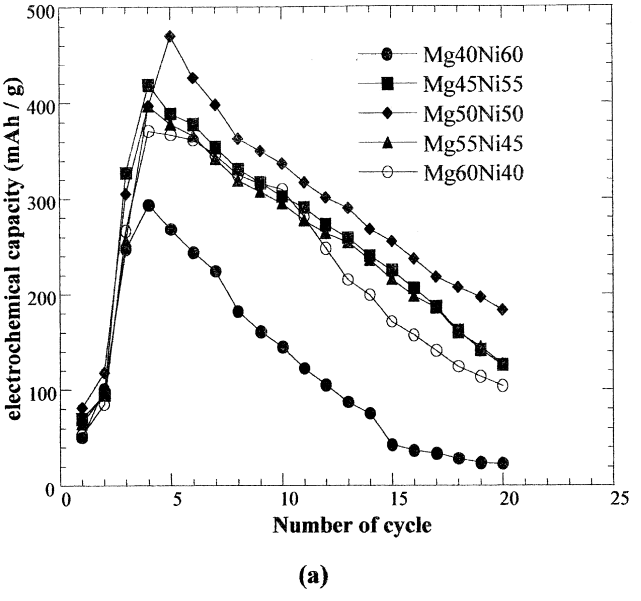


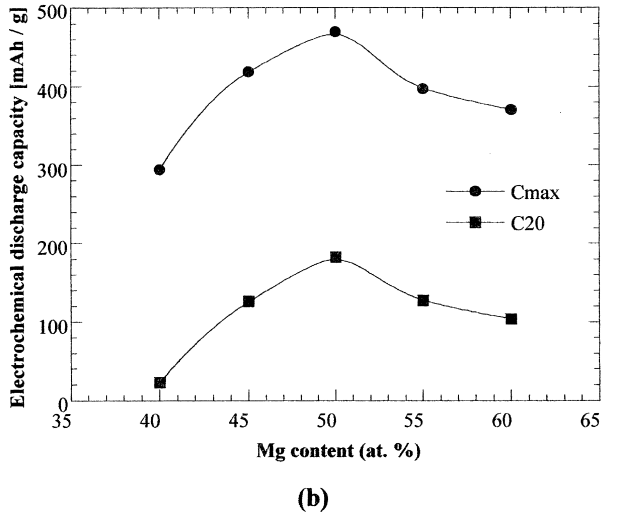


Fig. 4. (a) Variation of the electrochemical capacity versus the cycle number for the different synthesized samples and (b) variation of the electrochemical capacity (maximum capacity and after 20 cycles) as a function of the Mg atomic content.

content, of the maximum electrochemical capacity ($C_{max}$) and the electrochemical capacity after 20 cycles ($C_{20}$). The discharge capacity decrease after 20 cycles is equal to 92, 70, 61, 68 and 72%, respectively, for the 40, 45, 50, 55 and 60 Mg at.% sample contents. During the electrochemical reaction, we have formation of $Mg(OH)_2$ hydroxide on the surface of the grains, which prevents the diffusion of the hydrogen in the grain volume [16]. The thickness of this hydroxide layer increases when increasing the cycle number. Thus, the discharge capacity decreases when increasing the cycle number. At the same time, we think that the electrochemical capacities are not only a function of the amorphous phase proportion in the alloyed material but strongly influenced by the sample composition. In fact, the $Mg_{40}Ni_{60}$ sample had the lowest capacity while it had the highest amorphous phase proportion. $Mg_{50}Ni_{50}$ sample exhibits the best electrochemical capacity (470 mAh $g^{-1}$) with the lowest loss after 20 cycles (61%).

This electrochemical capacity is better than those obtained by Liu et al. [3] (350 mAh $g^{-1}$), Orimo et al. [4] (2.2 wt.%), Tarashita et al. [5] (1.8 wt.%) and Sun et al. [7] (336 mAh $g^{-1}$). Nohara et al. [8] obtained almost the same value (480 mAh $g^{-1}$) after 36 h of milling. Lenain et al. [6] obtained a better value of 500 mAh $g^{-1}$ when using a spex type ball mill during 80 h.

## 4. Conclusion

In this work, the following conclusions can be established: using milling conditions corresponding to a shock power of 6.49 W $g^{-1}$, we have successfully elaborated amorphous phase with very small quantity of residual Ni after 8 h 15 min, 8 h 25 min, 8 h 27 min, 9 h 10 min and 9 h 55 min for, respectively, 40, 45, 50, 55 and 60 Mg at.% content samples. These values are lower than that previously reported in the literature [3–5,7]. The best electrochemical capacity (470 mAh $g^{-1}$, equivalent of $MgNiH_{2.0}$) was reported for the sample $Mg_{50}Ni_{50}$ synthesized in about 8 h. Other alloyed samples $Mg_xNi_{100-x}$ for which compositions are different from $Mg_{50}Ni_{50}$ present lower electrochemical capacity values ranging from 294 to 419 mAh $g^{-1}$.

## Acknowledgements

The authors thank Audrey Miard for her participation in the material elaboration.

## References

[1] J.J. Reilly, R.H. Wiswall Jr., Inorg. Chem. 7 (1968) 2254.
[2] M. Abdellaoui, D. Cracco, A. Percheron-Guégan, J. Alloys Comp. 293–295 (1999) 501.
[3] W. Liu, H. Wu, Y. Lei, Q. Wang, J. Wu, J. Alloys Comp. 252 (1997) 234.
[4] S. Orimo, H. Fujii, K. Ikeda, Y. Fujikawa, Y. Kitano, J. Alloys Comp. 253–254 (1997) 94.
[5] N. Tarashita, M. Takahashi, K. Kobayashi, T. Sasai, E. Akiba, J. Alloys Comp. 293–295 (1999) 541.
[6] C. Lenain, L. Aymard, L. Dupont, J.-M. Tarascon, J. Alloys Comp. 292 (1999) 84–89.
[7] L. Sun, G.X. Wang, H.K. Liu, D.H. Bradhurst, S.X. Dou, Electrochem. Solid State Lett. 3 (3) (2000) 121.
[8] S. Nohara, K. Yamasaki, S.G. Zhang, H. Inoue, C. Iwakura, J. Alloys Comp. 280 (1998) 104.
[9] M. Abdellaoui, E. Gaffet, J. Alloys Comp. 209 (1994) 351.
[10] M. Abdellaoui, E. Gaffet, Acta Metall. Mater. 43 (3) (1995) 1087.
[11] A. Antoniadis, J. Berruyer, A. Filhol, Int. Rep. 87AN22T, Institut Lauë Langevin, Grenoble, 1998.
[12] E. Gaffet, M. Harmelin, J. Less-Common Met. 157 (1990) 201.
[13] G. Cocco, S. Enzo, S. Schiffini, L. Battezzati, Mater. Sci. Eng. 97 (1988) 43.
[14] K. Suzuki, J. Non-Cryst. Solids 112 (1989) 23.
[15] E. Gaffet, Mater. Sci. Eng. A 119 (1989) 185.
[16] W.H. Liu, Y.Q. Lei, D.L. Sun, J. Wu, Q.D. Wang, J. Power Sources 58 (1996) 243.